



## Low-loss optical waveguides for the near ultra-violet and visible spectral regions with Al<sub>2</sub>O<sub>3</sub> thin films from atomic layer deposition

Mustafa M. Aslan<sup>1</sup>, Nathan A. Webster, Courtney L. Byard, Marcelo B. Pereira<sup>2</sup>, Colin M. Hayes, Rodrigo S. Wiederkehr, Sergio B. Mendes\*

Department of Physics and Astronomy, University of Louisville, Louisville, KY, 40292, USA

### ARTICLE INFO

#### Article history:

Received 14 August 2009  
Received in revised form 26 February 2010  
Accepted 5 March 2010  
Available online 16 March 2010

#### Keywords:

Alumina film  
Aluminum oxide  
Atomic layer deposition  
Optical waveguide  
Propagation loss  
Ultra-violet  
Optical constants  
Refractive index

### ABSTRACT

In this work, we report low-loss single-mode integrated optical waveguides in the near ultra-violet and visible spectral regions with aluminum oxide (Al<sub>2</sub>O<sub>3</sub>) films using an atomic layer deposition (ALD) process. Alumina films were deposited on glass and fused silica substrates by the ALD process at substrate/chamber temperatures of 200 °C and 300 °C. Transmission spectra and waveguide measurements were performed in our alumina films with thicknesses in the range of 210–380 nm for the optical characterization. Those measurements allowed us to determine the optical constants ( $n_w$  and  $k_w$ ), propagation loss, and thickness of the alumina films. The experimental results from the applied techniques show good agreement and demonstrate a low-loss optical waveguide. Our alumina thin-film waveguides are well transparent in the whole visible spectral region and also in an important region of the UV; the measured propagation loss is below 4 dB/cm down to a wavelength as short as 250 nm. The low propagation loss of these alumina guiding films, in particular in the near ultra-violet region which lacks materials with high optical performance, is extremely useful for several integrated optic applications.

© 2010 Elsevier B.V. All rights reserved.

### 1. Introduction

The requirement of high sensitivity and extremely low limit of detection in biological and chemical sensors has directed the attention of several researchers to use single-mode integrated optic waveguides in place of attenuated total reflection elements; sensitivity enhancements of about five orders of magnitude are possible in single-mode integrated optic devices when compared to direct transmission measurements [1,2]. For these integrated optic applications and others, the guiding film must have very low propagation loss, which then requires excellent surface quality of the guiding film and substrate, high homogeneity in the film to avoid scattering, and low residual absorption in the spectral region of interest. In order to reach those conditions, a proper material and fabrication process are needed to deliver waveguide-quality films. Because of their high refractive index in the visible wavelength region, metal oxides (e.g. HfO<sub>2</sub>, Ta<sub>2</sub>O<sub>5</sub>, ZrO<sub>2</sub>, Nb<sub>2</sub>O<sub>5</sub>, and Corning glass 7059) are widely used as waveguide-based biological and chemical sensors [1–6]. In addition, metal oxides typically provide a chemically tunable interface as they have surface

properties (e.g. surface charge density) that can be conveniently modified by changing pH level of the aqueous solution covering the waveguide film.

Many intrinsic transition bands of biological materials (proteins, DNA, lipid bilayers, etc.) are located in the near ultra-violet (UV) region, and thus several potential applications of integrated optic waveguides as biological and chemical sensors reside in this spectral band. However, usual optical waveguides and their associated fabrication processes fail to reach adequate optical performance in this spectral region. It is highly needed to develop integrated optic devices that have adequate performance at shorter wavelengths than the usual infra-red (IR) and visible spectral regions. To reach optical waveguides with low-loss and high refractive index in the UV spectral region, a highly transparent material with a proper deposition process is required. For this purpose, aluminum oxide (or alumina, Al<sub>2</sub>O<sub>3</sub>) is a natural candidate to achieve those requirements. Alumina is an important material used in many bulky optical components because of its high transparency from the near-UV to the near infra-red regions. In addition, alumina thin films have also been used in integrated optic applications as optical waveguides for the telecommunication window around the 1.5- $\mu$ m band. However, typical alumina films from traditional fabrication techniques fail to reach adequate low propagation losses in the UV region. Propagation loss in optical waveguides is generally affected by four major defects in the guiding structure: discrete defects in the film (such as porosity, bubbles, or particles), surface roughness (either in the film or

\* Corresponding author. Tel.: +1 502 852 0908; fax: +1 502 852 8128.

E-mail address: [sbmend01@louisville.edu](mailto:sbmend01@louisville.edu) (S.B. Mendes).

<sup>1</sup> Current address: Materials Institute, TUBITAK Marmara Research Center, Gebze, Kocaeli, Turkey.

<sup>2</sup> Current address: Instituto de Física, UFRGS, Campus do Vale, CP 15051, 91501-970, Porto Alegre, RS, Brazil.

substrate), intrinsic absorption, and imperfect stoichiometry in the film [7]. Many of these defects can be related to the deposition processes. Deposition of alumina films are widely reported in the literature, but propagation losses of integrated optic devices are notoriously restricted to the visible (mostly at 633 nm) and IR regions. Regarding the fabrication of high quality alumina thin films for integrated optic applications, the major processes used are d.c. planar magnetron sputtering [8], r.f. sputtering [9], ion-beam sputtering [10], plasma-enhanced chemical vapor deposition (PE-CVD) [11], and pulsed laser deposition [12]. An early work by Este and Westwood [8] studied the fabrication conditions in a d.c. sputtering process for improving the optical properties of an alumina film; a propagation loss of about 1 dB/cm at 633 nm was reported for their optimum process. Later, Smit et al. [9] provided an investigation based on r.f. sputtering process to coat alumina films on oxidized silicon substrates; after an annealing process at 800 °C, the refractive index of their alumina film increased from 1.54 to 1.70 and the propagation loss decreased from 25 dB/cm to about 1 dB/cm, with both measurements collected at 633 nm. Arnold and Cole [10] showed that ion-beam sputtering could be used to produce high performance alumina films by pre- and post-annealing; they reported propagation loss at 633 nm of 0.4–2.9 dB/cm (before annealing) and 0.23 dB/cm (after annealing). Alumina waveguides by the PE-CVD were produced for applications in optical communications at the near IR region [11]; the propagation loss achieved at the 1.1–1.8  $\mu\text{m}$  region was about 0.2 dB/cm after annealing at 800 °C. As seen above, most of the alumina waveguides with low propagation loss were achieved when the films were either deposited at high temperature or annealed at high temperature. One exception is the pulsed laser deposition process, as reported in the work by Suarez-Garcia et al. [12] for the fabrication of amorphous alumina waveguides on silicon substrates at room temperature; their film had a propagation loss of 2.5 dB/cm at 633 nm and a refractive index of about 1.67. Lacking in all those reports is a study on the optical properties of the alumina films at wavelengths shorter than 633 nm, which is highly relevant for many waveguide-based biosensors.

Although there are several reports on the growth of alumina thin films by the atomic layer deposition (ALD) process [13], none of them so far has provided quantitative information on the optical performance of the alumina thin films for integrated optic applications. In particular, important pieces of information that are missing in the literature are the propagation loss and optical constants of those films over a broad spectral range. In this work, we focus to quantify thoroughly those key parameters in the visible and UV spectral regions. In general, atomic layer deposition (ALD) process has attracted the attention of several researchers due to some unique advantages over other deposition processes. For instance, in the ALD process, the thin film is grown through chemically covalent bonds at a self-limiting step of one atomic layer per cycle; this feature tends to form a smooth film surface required for many applications. It is also possible to use ALD to deposit high quality films [14] at a wide range of temperatures, including room temperature. The self-limiting nature of the process allows the growth of films that are conformal to the substrate surface with an excellent uniformity on the thickness and optical properties. Reproducibility in the thickness and optical properties of the deposited films is also very good, since each cycle creates one atomic layer on the substrate surface. Critical parameters for the ALD deposition process are chamber temperature, pressure, and purge-gas flow rate.

The goal of the present work is to create and characterize low propagation loss and high refractive index alumina films on fused silica and glass substrates for waveguide applications at the near-UV and visible spectral regions. We report here ALD films that were formed by sequentially exposing a working substrate to tri-methyl-aluminum (TMA) and H<sub>2</sub>O precursors to grow alumina films at

moderate deposition temperatures (200 °C and 300 °C). Optical transmission and coupling measurements were taken in order to characterize the optical properties (refractive index and propagation loss) of the deposited films. Grating couplers were used for coupling a light beam in and out of the thin film for waveguide mode measurements. Prior to the film deposition, two diffraction gratings (separated apart by 34 mm) were fabricated on the substrates to work as waveguide couplers, which greatly facilitated our measurements. Fabrication details of the integrated grating couplers can be found in the literature [15]. Atomic force microscope (AFM) images were also taken to inspect the topology and to quantify the surface roughness of the bare substrates and the deposited films.

## 2. Alumina (Al<sub>2</sub>O<sub>3</sub>) waveguide fabrication by atomic layer deposition (ALD)

Fused silica and glass substrates with dimensions of 75 mm × 25 mm × 1 mm were thoroughly cleaned to provide a pristine surface for the thin-film deposition. The substrates were then coated with an alumina thin film by using a Savannah-100 ALD from Cambridge NanoTech Inc. In order to form an alumina thin film, the ALD deposition process consists of alternating two precursors inside the vacuum reactor chamber: tri-methyl-aluminum (TMA from Sigma Aldrich) and de-ionized water (18 M $\Omega$ ). The TMA precursor is introduced into the reactor chamber for 25 ms, then the reactor chamber is purged with N<sub>2</sub> gas (20 sccm) for 8 s, which is followed by the introduction of the H<sub>2</sub>O precursor into the process chamber also for 25 ms, and finally the chamber is purged again with N<sub>2</sub> (20 sccm) for another 8 s. Those steps complete one full cycle that forms approximately one atomic layer on the substrate surface; by replicating the cycle described above at a certain number of times one can deposit a precise film thickness.

## 3. Characterization methods

In order to determine the optical constants ( $n_w$  and  $k_w$ ) and thickness ( $t_w$ ) of our ALD-deposited thin films of alumina, we have employed both the Envelope Technique (ET) [16,17] based on optical transmittance data and the Waveguide Mode Technique (WMT) [18–20].

### 3.1. Envelope Technique

The Envelope Technique is based on data from a transmission spectrum of a thin film deposited on a transparent substrate with parallel surfaces; the technique was originally developed by Manificier et al. [16] and later advanced by Swanepoel [17]. Transmission measurements are collected for an optical beam impinging almost perpendicularly to the film/substrate plane (the angle between the waveguide surface normal and the incident beam is 5°). By using films with thicknesses in the range of 200–400 nm, several interference fringes appear in the transmission spectrum at the visible and UV regions, as illustrated in Fig. 1 for one of our samples (alumina film deposited on fused silica substrate). Two envelope curves are then defined, one involving the maxima values ( $T_M$ ) and another one involving the minima values ( $T_m$ ) of the transmission curve. Those envelope curves form the basis for the calculations expressed in [17] to determine the refractive index, the extinction coefficient, the propagation loss, and the thickness of the thin film under investigation. The technique is particularly suitable for weakly absorbing films, ( $\frac{k_w}{n_w} \ll 1$ ), and assumes a homogeneous and isotropic thin film. As described in [17], the real part of the refractive index is given by:

$$n_w = \sqrt{A + \sqrt{A^2 - n_s^2}}, \quad (1)$$

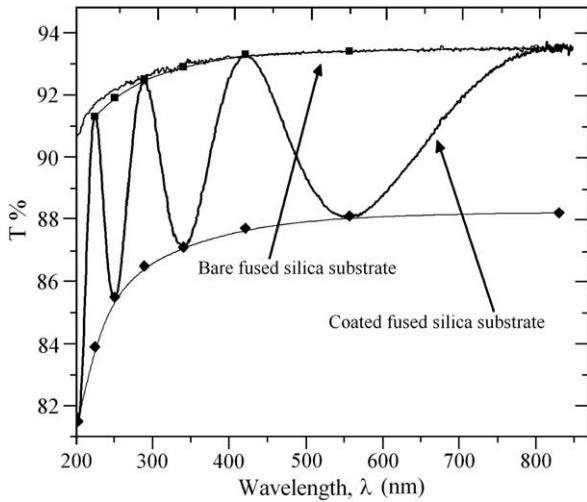


**Fig. 1.** The transmission spectrum of an alumina film coated on a fused silica substrate; the thickness of this particular alumina film was determined by the Envelope Technique to be  $(254 \pm 5)$  nm. For comparison, the plot also includes the transmission spectrum of a bare fused silica substrate.

where  $n_s$  is the refractive index of the substrate and the term  $A$  is defined by:

$$A \equiv 2n_s \frac{T_M - T_m}{T_M T_m} + \frac{n_s^2 + 1}{2}. \quad (2)$$

It is implicitly assumed in the previous Eqs. (1) and (2) that the medium surrounding the film/substrate sample is air, which is the usual case. By applying Eqs. (1) and (2), the refractive index of the film is calculated at each wavelength  $\lambda_m$  corresponding to an extreme value (either a maximum or a minimum) in the transmittance curve. Next, the thickness of the film is determined by using data from two consecutive minima or two consecutive maxima according to the following relation:

$$t_w = \frac{\lambda_m \lambda_{m+2}}{2(\lambda_m n_{m+2} - \lambda_{m+2} n_m)}. \quad (3)$$

The expression above allows for the calculation of the thickness from several pairs of data points; such redundancy is quite helpful as the average of those results substantially improves the estimated value for the film thickness. Then, the averaged value of the film thickness  $t_w$  is used to determine the order of each interference fringe:

$$m = \frac{4n_m \bar{t}_w}{\lambda_m}. \quad (4)$$

Those fringe orders  $m$  should in principle be integer numbers, but due to experimental errors they typically depart a little. It is well known that these integer numbers increase sequentially by one unit, when counting each fringe order from long to short wavelengths. In addition, the fringe orders must correspond to an even number at the locations where the envelope curve approaches the transmittance of a bare substrate. With such information in hand, we can round-off the experimental fringe orders to the appropriate integer order number. As explained in Swanepoel [17], this process of rounding-off the fringe orders improves substantially the estimated value of the film thickness by inverting Eq. (4) to solve for the film thickness at each extreme wavelength value. Averaging again those several results of the thickness give a much further improved estimation of the film thickness. And finally, Eq. (4) is used to solve for the refractive index

of the film based on the measured wavelength of an extreme value in the transmittance spectrum, the corresponding integer value of the fringe order, and the averaged film thickness.

Once the value for  $n_w$  and  $t_w$  have been determined, a solution for the extinction coefficient  $k_w$  is then possible from the following equation:

$$\exp(-\alpha_w t_w) = \frac{B - \sqrt{B^2 - (n_w^2 - 1)^3 (n_w^2 - n_s^4)}}{(n_w - 1)^3 (n_w - n_s^2)}, \quad (5)$$

where  $B \equiv 4n_w^2 n_s \left( \frac{T_M + T_m}{T_M T_m} \right)$  and  $\alpha_w$ , which is the absorption coefficient of the film, is given by  $\alpha_w \equiv \frac{4\pi k_w}{\lambda}$ . Once  $\alpha_w$  is determined from Eq. (5) using the experimental data, the extinction coefficient is then simply calculated by:

$$k_w = \alpha_w \frac{\lambda}{4\pi}. \quad (6)$$

From the analysis above, the thickness,  $\bar{t}_w$ , and the optical constants,  $n_w$  and  $k_w$ , of an alumina film were determined over a broad range of wavelengths, which is particularly important to construct a dispersion curve for the film under investigation. The transmittance spectra measurements of alumina thin films were taken with a Cary-300 spectrophotometer (Varian Inc.) in the wavelength range of 900 nm to 200 nm, which covers the transparency region of the fused silica substrates in the visible and UV ranges. Transmission data points were acquired at steps of 0.25 nm with a spectral resolution bandwidth of 0.5 nm and an integration time of 1 s. As already mentioned, Fig. 1 shows a typical transmittance spectrum (200–900 nm) of an alumina film coated on a fused silica substrate and also for comparison of a bare fused silica substrate.

### 3.2. Waveguide Mode Technique

The Waveguide Mode Technique was employed to further characterize the alumina films. An alumina film deposited on fused silica or glass substrate can confine guided modes when the film thickness exceeds a certain cut-off value. By measuring the effective refractive index of two (or more) guided modes of different mode orders or/and different polarizations (transverse electric, TE, or transverse magnetic, TM), one can retrieve the real part of the refractive index and the thickness of the guiding film [18–20]. To measure the effective refractive index of a planar waveguide formed by the substrate/alumina/air structure, a pair of periodic surface corrugation (diffraction grating) was created on the substrate surface prior to the deposition of the alumina film, as shown in Fig. 2. Then, after the alumina film has been deposited by the ALD process, we measured the coupling angle that the grating coupler could excite

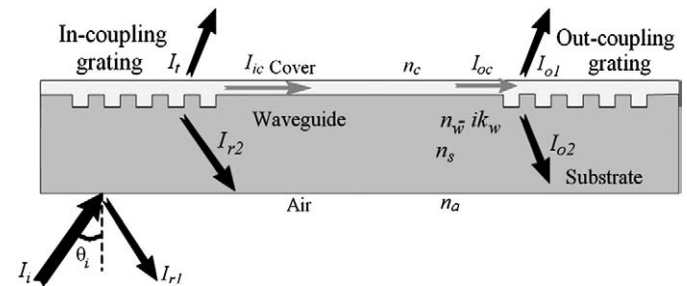


**Fig. 2.** The optical beams that were experimentally measured (drawn in black) and used to determine the in-coupled and out-coupled optical beams (drawn in gray). From those intensity measurements, the propagation loss could be determined for the single-mode integrated optical waveguide structure consisting of a cover medium, a guiding thin film, and a substrate.

guided modes on the waveguide structure at each polarization and at each allowed guided mode. Coupling of an optical beam from free space into a waveguide mode occurs when the effective refractive index of the waveguide,  $N_{\text{eff}}$ , is matched by the sum of the grating contribution plus the Snell's term, which is mathematically given by:

$$N_{\text{eff}} = p \frac{\lambda}{\Lambda} + n_a \sin \theta_{\text{in}}, \quad (7)$$

where,  $\lambda$  is the vacuum wavelength,  $\Lambda$  is the grating period,  $p$  is the grating diffraction order,  $n_a$  is the refractive index of air, and  $\theta_{\text{in}}$  is the incident angle between the incident beam and the normal to the waveguide surface.

The effective refractive index of a planar waveguide,  $N_{\text{eff}}$ , is related to the optical parameters in the structure through the dispersion relation given by:

$$\frac{2\pi}{\lambda} t_w \sqrt{n_w^2 - N_{\text{eff}}^2} + \phi_c + \phi_s = 2\pi m, \quad (8)$$

where  $m$  is the order of the waveguide mode, and the terms  $\phi_c$  and  $\phi_s$  are the phase shifts defined by:

$$\phi_c \equiv -2 \tan^{-1} \left[ \left( \frac{n_w}{n_c} \right)^{2\rho} \left( \frac{N_{\text{eff}}^2 - n_c^2}{n_w^2 - N_{\text{eff}}^2} \right)^{1/2} \right] \quad (9)$$

and

$$\phi_s \equiv -2 \tan^{-1} \left[ \left( \frac{n_w}{n_s} \right)^{2\rho} \left( \frac{N_{\text{eff}}^2 - n_s^2}{n_w^2 - N_{\text{eff}}^2} \right)^{1/2} \right], \quad (10)$$

where  $\rho = 0$  applies for the TE polarization, and  $\rho = 1$  applies for the TM polarization.

An experimental setup was built to measure coupling angles, and thus the effective refractive indices, with high accuracy and precision for both TE and TM polarizations. For this purpose, a high performance rotational stage (Danaher FIR) was used with a digital reader (Quadra-check 100 from Metronics). The waveguide was located at the center of rotational stage in vertical position. The light sources used in our experiments were: a 12-mW He–Ne laser from Thorlabs Inc, a tunable 40-mW argon-ion laser from Melles Griot, and a 20-mW He–Cd laser at 325 nm from Kimmon. The laser polarization was filtered by a linear polarizer before it was loosely focused on the grating via a long-focal-length lens (Thorlabs-AC254-300-A1). The rotational stage, which was initially set to zero by back-reflection, was rotated until the strongest coupling signal was found in a photodetector controlled by a power meter. Angle readings were recorded with better than 3-digit precision. The incident angles were measured for TE<sub>0</sub> and TM<sub>0</sub> modes, which then allowed the determination of thickness and refractive index of the film by numerically solving Eqs. (7)–(10).

Propagation loss was also measured using the pair of gratings integrated on the planar optical waveguide structure, as shown in Fig. 2. Propagation loss data on the waveguide could be determined by measuring the in-coupled and out-coupled intensities of the optical beam. As indicated in Fig. 2, the in-coupled intensity is given by

$$I_{\text{ic}} = I_i - (I_t + I_{r1} + I_{r2}), \quad (11)$$

and the out-coupled intensity is given by

$$I_{\text{oc}} = I_{o1} + I_{o2}. \quad (12)$$

In the equations above,  $I_i$  is the incident intensity,  $I_t$  is the transmitted intensity,  $I_{r1}$  and  $I_{r2}$  are the reflected intensities from the front and back surfaces respectively, and  $I_{o1}$  and  $I_{o2}$  are the intensities of the

out-coupled beams from the exit grating coupler. Propagation loss, in units of dB, can then be calculated from Eqs. (11) and (12) as:

$$\text{Loss} = -10 \log \left( \frac{I_{\text{oc}}}{I_{\text{ic}}} \right) = -10 \log \left[ \frac{I_{o1} + I_{o2}}{I_i - (I_t + I_{r1} + I_{r2})} \right]. \quad (13)$$

### 3.3. Alumina roughness

Surface roughness at the boundaries of the waveguide film (top and bottom interfaces) can potentially scatter a propagating guided mode and be a source of optical attenuation. An atomic force microscope (Autoprobe-M5, Park Instruments) was used to check surface topologies of both the ALD-deposited films and the uncoated substrates. AFM measurements were performed in contact mode in an area of  $5 \times 5 \mu\text{m}^2$ . Since surface roughness is approximately independent of the film thickness, only alumina films with thickness of 380-nm were scanned at 4 different locations. The root mean square of the surface roughness was 1.25 nm for the bare fused silica substrate and 0.95 nm for the alumina film coated on the fused silica substrate. Lower surface roughness and varying topologies were observed on the coated substrates. The average surface roughness for a bare glass substrate and an alumina film coated on a glass substrate were 0.62 nm and 0.52 nm, respectively. Regardless of the substrate type, our AFM results indicate that the amount of surface roughness on the top surface of the waveguide film is slightly less than the buried interface between the film and the substrate, which demonstrates that the ALD process at least maintains the roughness of the substrate, if not improving it. Such feature is quite relevant to keep the propagation losses of the IOW at low levels.

## 4. Results and discussions

In this work, four different alumina film thicknesses were deposited onto glass and fused silica substrates. The thicknesses of our films, as determined by the Envelope Technique, were  $210 \pm 5$ ,  $254 \pm 5$ ,  $322 \pm 2$ , and  $380 \pm 2$  nm. In particular, the thicker waveguides (254, 322 and 380 nm) provide several interference fringes (maximum and minimum in the transmittance curve) in the visible and near-UV spectral regions, and thus increase the accuracy of the calculations by the Envelope Technique. On the other hand, the 210-nm thick waveguide film provides a single-mode structure (one TE<sub>0</sub> and one TM<sub>0</sub>) at the spectral range of interest, and thus several samples with this nominal thickness were prepared for the application of the Waveguide Mode Technique.

The reactor chamber temperature was kept constant for all depositions at either 200 °C or 300 °C, where a high refractive index is expected [14]. Deposition rate curves for these two temperatures ( $T_{\text{rc}}$ ) of the reaction chamber are shown in Fig. 3. By applying a linear curve-fit to our measurements, we obtained a deposition rate of 1.013 Å/cycle for  $T_{\text{rc}} = 300$  °C and 1.090 Å/cycle for  $T_{\text{rc}} = 200$  °C, which shows that lowering the substrate temperature slightly increases the deposition rate of alumina per cycle. However, the variation of the ALD deposition rate is small because of the self-limiting nature of the ALD process. In one report [21], deposition rates of alumina using the ALD process were reported in the range of 0.8 to 1.1 Å/cycle depending on process parameters such as temperature, exposure time, purge time, purge-gas flow rate, and chamber pressure. In another report [22], the deposition rate was reported to be approximately 1.1 Å/cycle for a reactor temperature of 177 °C and exposure times of 0.33 s for TMA and water. Others have also observed [23] that small variations in the deposition rate can occur when the chamber temperature is changed, but our thickness and refractive index measurements show that it was within an acceptable temperature window where the condition for single atomic layer deposition was satisfied.

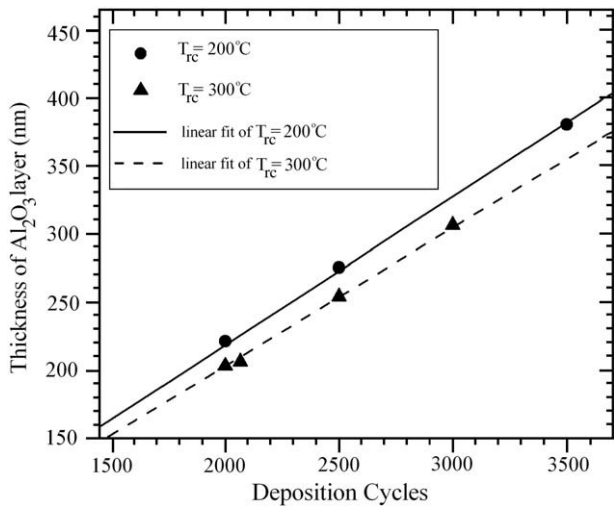


Fig. 3. Alumina film thickness as a function of number of cycles in the ALD process at different temperatures of the reactor chamber,  $T_{rc}=200\text{ }^{\circ}\text{C}$  and  $300\text{ }^{\circ}\text{C}$ . Slope of the curves provides the deposition rate of the ALD process at each temperature.

The real part of the refractive index of our alumina waveguide films,  $n_w$ , at different wavelengths was determined by the Envelope and Waveguide Mode Techniques, and the experimental results are summarized in Fig. 4. As previously mentioned, the Envelope Technique results were collected over 4 samples with different thicknesses and the Waveguide Mode Technique results reflect an average over 10 data samples with a thickness of approximately 210 nm. These data correspond to films that were coated at  $300\text{ }^{\circ}\text{C}$  for the reactor chamber temperature. A Cauchy expression was used to fit the experimental results [24]. The plotted graph shows that the alumina waveguide film has a high refractive index and a strong dispersion, especially around the near-UV range. The  $n_w$  is about 1.64 at 850 nm and it increases with decreasing wavelength to 1.86 at 200 nm. By using the multiple lines of an argon-ion laser, the coupling angles at different wavelengths ranging from 454 nm to 514 nm were measured for different waveguide modes so we could apply the Waveguide Mode Technique to determine the real part of the alumina film refractive index. In Fig. 4, the consistency can be seen between the two characterization approaches we have used.

Next, we focused on the determination of the extinction coefficient of the film,  $k_w$ , which can quantify how much light is absorbed and/or

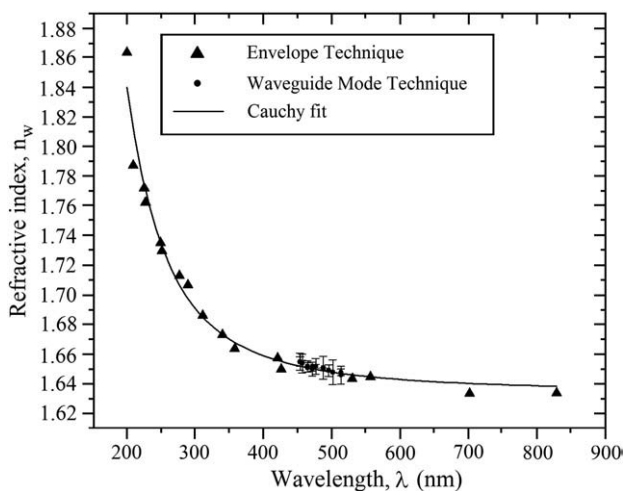


Fig. 4. Real part of the refractive index of the alumina thin film as determined by the Envelope and Waveguide Mode Techniques.

scattered by defects in the alumina film. For this purpose, transmittance data taken at three different spots from the three thicker films deposited on fused silica substrates were analyzed. By using the Envelope Technique, the extinction coefficient,  $k_w$ , was determined as a function of wavelength according to Eqs. (5) and (6); our experimental results are shown in Fig. 5. As the data indicates, the extinction coefficient of the alumina film in the spectral range from 250 nm to 650 nm is quite low and demonstrates that the alumina thin film, as prepared by the ALD process, shows very low loss even in the near-UV region. There is a large region in the UV region and visible spectrum with low  $k_w$  values, which quantifies a highly transparent film that can be useful for several applications. In addition, we observe that the current data shows a sharp increase in the extinction coefficient for wavelengths smaller than 230 nm, as it approaches the alumina absorption band.

Propagation losses measurements were determined using the Waveguide Mode Technique, as previously described in connection with Fig. 2 and summarized in Eq. (13). The WMT loss measurements were taken via grating couplers (one for input, another for output) for 12 samples at the 543-nm and 633-nm wavelengths. The average results from the  $TE_0$  mode, which were  $(1.1 \pm 0.3)$  dB/cm at 633 nm and  $(2.0 \pm 0.7)$  dB/cm at 543 nm, agree well with the results from the  $TM_0$  modes  $(1.3 \pm 0.5)$  dB/cm at 543 nm. Besides the WMT direct determination just described, the Envelope Technique can also be used to estimate the propagation loss in a waveguide if one assumes that the dominant factor for the optical losses of a beam propagating inside the waveguide is originated from the extinction coefficient of the guiding film. In this case, the propagation loss can be evaluated from the extinction coefficient through the following equation:

$$Loss = -10 \log \left( e^{-4\pi \frac{k_w l}{\lambda}} \right) = \frac{10 \times 4\pi k_w l}{\lambda \ln(10)} \quad (14)$$

where  $l$  is the distance between the input and output grating couplers. The average values and standard deviations of the ET measurements were taken from three samples of different thicknesses (254, 322, and 380 nm) and each sample was measured at 3 different spots of the alumina coated fused silica substrates. The experimental results of the propagation loss per-unit-length (dB/cm) for all techniques described above are shown in Fig. 6. The ET experimental results span over the 208–633 nm spectral region and show good agreement with the WMT technique at the long wavelengths range and very low propagation losses down to 250 nm, even though the standard deviations of the losses are not so small at some wavelengths in the UV region. Our

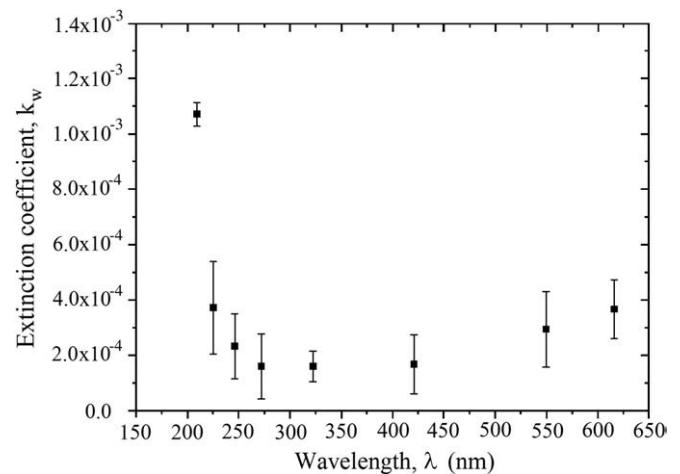


Fig. 5. Imaginary part of the refractive index (extinction coefficient) of the alumina thin film as experimentally determined by the Envelope Technique.

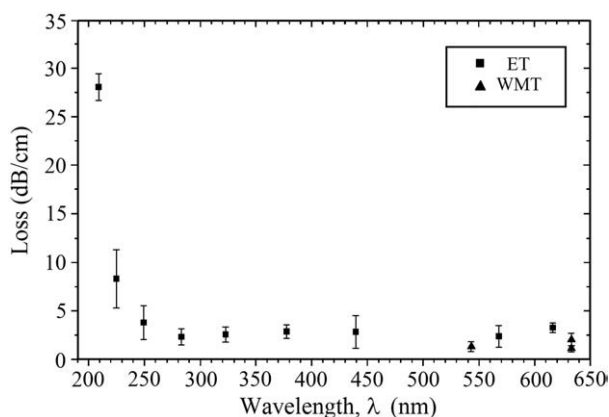


Fig. 6. Propagation loss of the alumina thin film waveguide as a function of wavelength as measured by the Envelope and Waveguide Mode Techniques.

experimental results at 633 nm were  $(1.1 \pm 0.3)$  dB/cm by the Waveguide Mode Technique and 2.6 dB/cm by the Envelope Technique, which seems to indicate that the assumption underlying the ET calculations is over-estimating the contribution of the extinction coefficient for evaluating the propagation loss; a direct and straightforward measurement of the propagation loss as provided by the Waveguide Mode Technique consistently gave us a lower value. We also note that our results of the propagation loss at 633 nm are similar to the best results existent in the literature, which were typically obtained at high temperatures of annealing or deposition. More remarkably, the present work demonstrates that the ALD alumina films can reach the important UV spectral region, which was not addressed in previous studies. Fig. 7 shows a picture of our alumina thin-film waveguide when a 325-nm UV laser beam propagates for 34 mm inside the single-mode structure and out-couples from a grating coupler. Strong out-coupling qualitatively and visually corroborates the previously discussed quantitative measurements of low propagation loss in our ALD-deposited alumina films. These experimental results confirm the ability of the ALD process to produce low-loss optical waveguides well inside the UV region; such ability is expected to become extremely useful for developing integrated optic devices in the near-UV and visible spectral regions for a variety of applications including sensing of many relevant biological materials (e.g., see [25] for specific applications).

## 5. Conclusions

In summary, we report here the fabrication and characterization of single-mode integrated optical waveguide with low propagation loss in near-UV and visible spectral regions from alumina thin films deposited by the atomic layer deposition (ALD) process. Glass and fused silica substrates were coated with film thickness in the range of

210–380 nm. The optical characterization of the waveguides was performed by the Envelope Technique and the Waveguide Mode Technique. Optical constants and propagation losses were calculated for several samples and for a broad spectral range, 200–633 nm. A highly transparent single-mode optical waveguide is reported to reach a wavelength as short as 250 nm. Such experimental results will certainly enable the fabrication of several integrated optic devices in the short wavelength spectral region for a variety of applications. In particular, our group has already started exploiting the high quality of ALD-deposited alumina waveguides and we have incorporated those films as part of a single-mode integrated optical waveguide platform for spectroscopic studies of surface-adsorbed protein sub-monolayers [25].

## Acknowledgments

This work was supported by the National Institute of Health (award # RR022864 and R01EB007047 to SBM) and the National Science Foundation (award # DBI 0359442 to SBM).

## References

- [1] S.B. Mendes, L.F. Li, J.J. Burke, J.E. Lee, D.R. Dunphy, S.S. Saavedra, *Langmuir* 12 (1996) 3374.
- [2] D. Kelly, K.M. Grace, X. Song, B.I. Swanson, D. Frayer, S.B. Mendes, N. Peyghambarian, *Opt. Lett.* 24 (1999) 1723.
- [3] J.S. Martinez, W.K. Grace, K.M. Grace, N. Hartman, B.I. Swanson, *J. Mater. Chem.* 15 (2005) 4639.
- [4] H. Mukundan, J.Z. Kubicek, A. Holt, J.E. Shively, J.S. Martinez, K. Grace, W.K. Grace, B.I. Swanson, *Sens. Actuators, B, Chem.* 138 (2009) 453.
- [5] J. Voros, J.J. Ramsden, G. Csucs, I. Szendro, S.M. De Paul, M. Textor, N.D. Spencer, *Biomaterials* 23 (2002) 3699.
- [6] A. Peled, A. Chiasera, M. Nathan, M. Ferrari, S. Ruschin, *Appl. Phys. Lett.* 92 (2008) 221104.
- [7] J.M. Mir, J.A. Agostinelli, *J. Vac. Sci. Technol., A* 12 (1994) 1439.
- [8] G. Este, W.D. Westwood, *J. Vac. Sci. Technol., A* 2 (1984) 1238.
- [9] M.K. Smit, G.A. Acket, C.J. Vanderlaan, *Thin Solid Films* 138 (1986) 171.
- [10] S.M. Arnold, B.E. Cole, *Thin Solid Films* 165 (1988) 1.
- [11] M. Mahnke, S. Wiechmann, H.J. Heider, O. Blume, J. Muller, *AEU, Int. J. Electron. Commun.* 55 (2001) 342.
- [12] A. Suarez-García, J. Gonzalo, C.N. Afonso, *Appl. Phys., A Mater.* 77 (2003) 779.
- [13] S.M. George, A.W. Ott, J.W. Klaus, *J. Phys. Chem.* 100 (1996) 13121.
- [14] M.D. Groner, F.H. Fabreguette, J.W. Elam, S.M. George, *Chem. Mater.* 16 (2004) 639.
- [15] C.M. Hayes, M.B. Pereira, B.C. Brangers, M. M. Aslan, R. S. Wiederkehr, J.H. Lake, and S.B. Mendes, 2008 17th Biennial University/Government/Industry Micro-Nano Symposium, Louisville, KY, U.S.A., July 13–16 (2008) 227.
- [16] J.C. Manificat, J. Gasiot, J.P. Fillard, *J. Phys. E Sci. Instrum.* 9 (1976) 1002.
- [17] R. Swanepoel, *J. Phys. E Sci. Instrum.* 16 (1983) 1214.
- [18] P.K. Tien, *J. Opt. Soc. Am.* 60 (1970) 723.
- [19] P.K. Tien, *Appl. Opt.* 10 (1971) 2395.
- [20] R. Ulrich, R. Torge, *Appl. Opt.* 12 (1973) 2901.
- [21] S.J. Yun, K.H. Lee, J. Skarp, H.R. Kim, K.S. Nam, *J. Vac. Sci. Technol., A* 15 (1997) 2993.
- [22] A.W. Ott, J.W. Klaus, J.M. Johnson, S.M. George, *Thin Solid Films* 292 (1997) 135.
- [23] D.R.G. Mitchell, G. Triani, D.J. Attard, K.S. Finnie, P.J. Evans, C.J. Barbe, J.R. Bartlett, *Smart Mater. Struct.* 15 (2006) S57.
- [24] D. Poelman, P.F. Smet, *J. Phys. D, Appl. Phys.* 36 (2003) 1850.
- [25] R.S. Wiederkehr, G.C. Hoops, M.M. Aslan, C.L. Byard, S.B. Mendes, *J. Phys. Chem., C* 113 (2009) 8306.

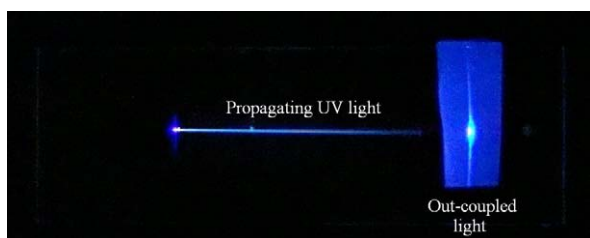


Fig. 7. Picture of the guided UV light (325 nm) showing the out-coupled m-line after the optical beam has propagated 34 mm inside the single-mode alumina thin-film optical waveguide.